SIMULATION OF THE JAVA SEA
USING AN OCEANIC GENERAL CIRCULATION MODEL

Ibnu Sofian

Balai Penelitian Geomatika
Badan Koordinasi Survei dan Pemetaan Nasional

ABSTRACT

The Hybrid Coordinate Ocean Model (HYCOM) is used to simulate the Java Sea mean sea level, surface current and volume transport. The model (JSD, Java Sea Domain) is driven by the European Remote Sensing (ERS) satellite-derived and National Center Environmental Prediction (NCEP) wind stresses. The ERS-derived and NCEP wind speeds and stresses are compared to investigate the impacts of the different wind forcing data on the estimation of the Java mean sea level. The validation results illustrate that the simulated mean sea levels agree well with the tide gauge sea levels. The NCEP wind-driven JSD (called NJSD) model has correlation coefficients from 0.53 to 0.84 and root mean square errors (RMSE) of 47 mm to 76 mm. On the other hand, the ERS wind-driven JSD (Called EJSD) model has the correlation coefficients from 0.71 to 0.89 and RMSEs of 40 mm to 61 mm against tide gauge sea level, respectively. These validation results reveal that accuracy of the EJSD model is better than the NJSD model.

The relationship between the Java Sea zonal wind and volume transport is also investigated by using HYCOM. Due to the shallowness of the Java Sea, the volume transport is dominated by the wind, which is greatly different between ERS and NCEP. The Java Sea volume transport is directed eastward and westward during the northwest (October to March) and southeast (April to September) monsoons, respectively. The westerly and easterly ERS wind stresses in December and August are 0.01 N/m^2 and 0.03 N/m^2 higher than NCEP wind stresses, respectively. Moreover, the NCEP mean wind speed is 1.0 m/s and 2.5 m/s lower than ERS mean wind speed, during the northwest and southeast monsoons, respectively. Consequently, the Java Sea eastward volume transport simulated by the EJSD model is found to be larger than the one simulated by the NJSD model. The EJSD model-simulated Java Sea eastward and westward volume transports in December and August are 0.23 Sv and 0.30 Sv larger than the ones simulated by the NJDS model, respectively.

Key words: Java Sea, ERS wind, NCEP wind, HYCOM.

INTRODUCTION

The location of the Java Sea and the Makassar Strait is depicted in Figure 1. The Java Sea has average depths from 40 m to 50 m. The Java Sea is bordered by the Kalimantan Island to the north, the Java Island on the south, the Sumatra Island on the west, the southern Makassar Strait on the east, the Karimata Strait on the northwest, and the Sunda Straits on the southwest.

Many studies on the Indonesian troughflow (ITF) have been conducted through the Arlindo (Arus Lintas Indonesia, [1,2,3]) project and others. Unfortunately, most of the scientists neglected what was happening in the Java Sea due to its shallowness [4]. The past observation [5] and NCEP wind-driven ocean model results [6,7] show that the Java Sea low-salinity surface water shifts into the southern Makassar Strait during the northwest monsoon from October to March. The southeast monsoon winds return the low-salinity water back into the Java Sea during the southeast monsoon from April to September. Sofian et al. [6] also argue that the strong westward volume transport generates high sea level within the Java Sea. Moreover, the Java Sea transport is directed eastward during the northwest monsoon, from October to March, and to the westward during the southeast monsoon from April to September, following the monsoonal wind-indu

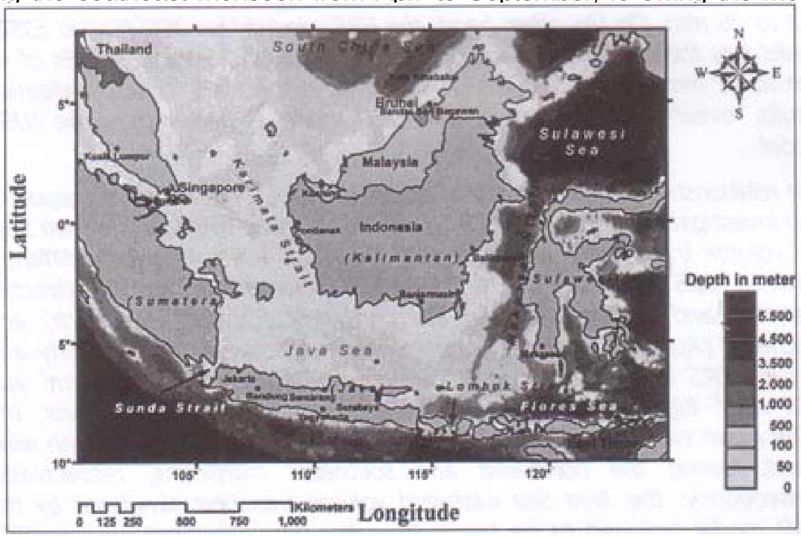

Figure 1: Bathymetric map of the Indonesian Sea, including the Sunda, and Karimata Straits, the South China Sea, the Java Sea, the Makassar Strait, the Flores Sea, and the Sulawesi sea.

The aim of this study is to investigate the impacts of different wind forcing data on the simulation accuracy of the Java Sea. The models are forced by the ERS and NCEP winds. The ERS wind has a limitation on the period of data, which is only available from 1992 to 2001, while the NCEP wind is available from January 1948 to the present. However, the NCEP wind has the limitation on the spatial resolution of 1.875° longitude yxJ latitude, while the ERS wind has the spatial resolution of 1° longitude and latitude. '-e present study addresses the following questions: 1) how good is the modelled mean sea level against the tide gauge mean sea level?, 2) are the modelled mean sea levels eiable to express the El Nino Southern Oscillation (ENSO) impacts on the mean sea evel?, and 3) can the different wind forcing change the Java Sea volume transport?

This paper is organized as follows. The brief explanation of data used in this earch and the model configuration are given in the section of Ocean Model. The Description of tide gauge mean sea level data and results of model validation are described in the section of Model Validation. The wind patterns and the climatology over the Java Sea are described in the section of Wind Climatology. The relationship between wind and -xxJelled surface current during the northwest and southeast monsoons are discussed in ne section of Wind and Surface Currents. The climatology of the Java Sea volume transport is described in the section of Java Sea Volume Transport. The final section is -stained to concluding remarks.

Ocean Model

HYbrid Coordinate Ocean Model (HYCOM) [8] is applied to simulate the Java Sea and the Makassar Strait. The model region is the Indonesian Sea including the Southern South China Sea, the Java Sea, the Sulawesi Sea, the Karimata Strait, and the Makassar Strait, as shown in Figure 1. The horizontal grids span from 80°E to 125°E and from 10°S to 8°N. This domain is referred to as the Java Sea Domain (JSD) hereafter, and the grid resolution is Mercator 0.1° longitude and latitude. The model is configured with 22 layers,and the bottom topography is based on ETOP02 data. This model uses KPP (K-ProfileParameterization) vertical mixing, and the explanation of the method can be found in [9]. More detail description of the HYCOM equations and numerical algorithms can be found in [8]. The model relaxes at the lateral boundaries to the World Ocean Atlas (WOA) 1998 monthly climatology, which contains salinity and temperature profiles. Tidal forcing is not available in HYCOM. The model is driven by weekly ERS and NCEP wind speed and stress data. The ERS wind data are derived from Centre ERS d'Archivage et de Traitement -Institut francais de recherche pour l'exploitation de la mer (CERSAT-IFREMER [10]). The ERS wind has the spatial resolution of 1° longitude and latitude. The atmospheric forcing that contains surface air temperature, surface specific humidity, net shortwave and longwave radiations, and precipitation are based on the NCEP reanalysis data. The weekly NCEP data are calculated from the daily mean data. The NCEP data have the spatial resolution of the Gaussian grid 1.875° longitude and latitude. The model's sea surface temperature (SST) is the National Oceanic and Atmospheric Administration (NOAA) optimal interpolation (01) SST. The NJSD and EJSD model are nested to the large domain model, which covers the area from 30°E to 60°W and from 45°S to 45°N. This region is referred to as the Indo-Pacific Ocean Domain (IPD). The ERS and NCEP wind-driven IPD models a'e called EIPD and NIPD models, respectively. NIPD and EIPD models have 1° longitude nd latitude grid spacing. Moreover, the EIPD and NIPD models use the same topography iata and parameters of the forcing fields, initial conditions, and mixing layer model as used in the EJSD and NJSD models, respectively.

The sensible and latent heat fluxes are calculated during model runs, using the model SST and the bulk formulae. The NJSD and EJSD models are relaxed to the NIPD and EIPD models, respectively. The relaxation time scale increases from 0.1 to 3 days with distance away from the boundaries. The precipitation and evaporation are also included in this model. The summary of model configurations is presented in Table 1.

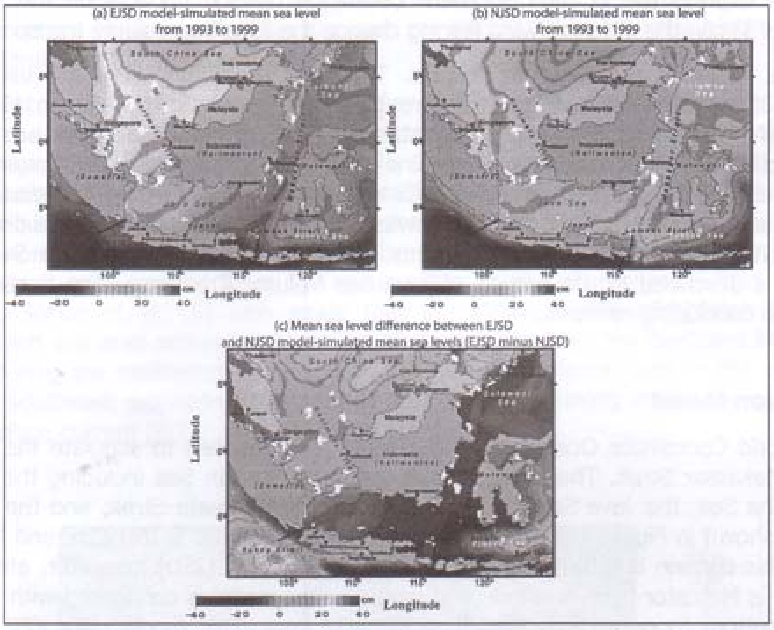

Figure 2: Simulated mean sea levels for 7 years based on (a) EJSD and (b) NJSD, and (c) mean sea level difference between EJSD and NJSD-simulated sea levels from 1993 to 1999.

Table 1 : EJSD and NJSD model Figurations.

No	Parameter	Description	Comments
1	Geographical area	100°E to 125°E and from 10°S to 8°N	
2	Operational mode	Hind-cast	
3	Model run	from 1 January 1993 to 31 December 1999	
4	Nestinq conditions	on	In EIPD and NIPD models
5	Grid size	251 x 181	
6	Spatial resolutions	10 km x 10 km	
7	Layer	22 layers	
8	Time step baroclinic	200 seconds	
9	Time step barotropic	10 seconds	
10	Relaxation	WOA 1998	
11	Forcing fields	NCEP reanalysis II	Weekly, based on daily mean
12	Wind Forcing	ERS and NCEP wind stresses	ERS for EJSD and NCEP for NJSD
13	Topography	ETOP0 2	
14	Vertical mixing	KPP	
15	Tidal forcing	Not available in HYCOM	
16	River forcing	off	
17	SST forcing	Weekly OI SST from NOAA	weekly

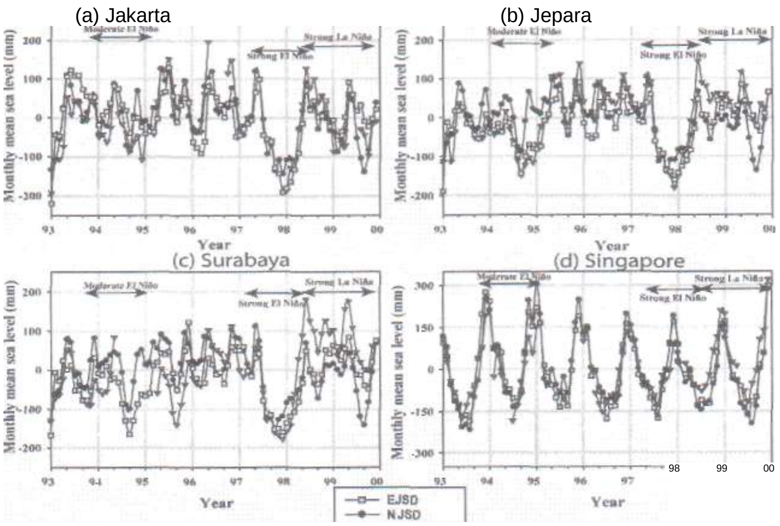

Figure 3: Time series of tide gauge, NCEP and ERS winds driven ocean model simulated sea levels at Jakarta, Jepara and Surabaya and Singapore. The mean sea levels are relative to 7 years mean, from 1993 to 1999.

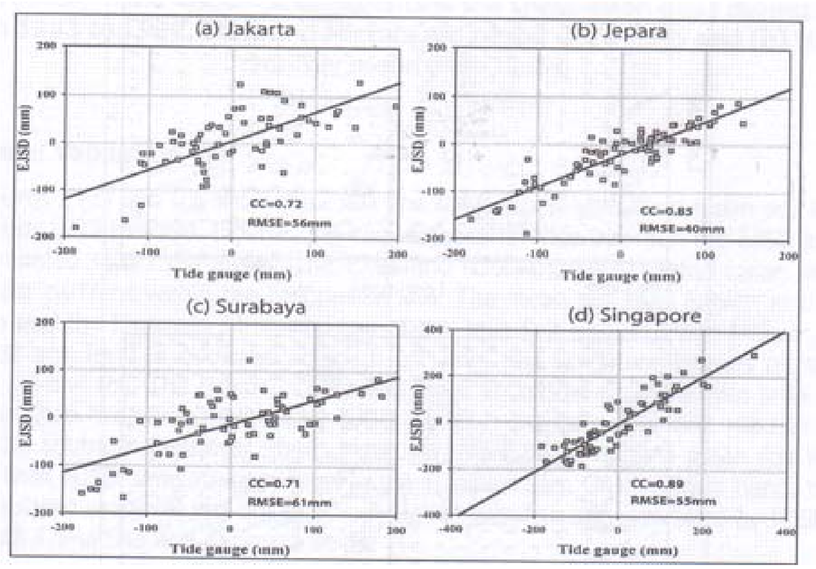

Figure 4: The scatter plot of the comparison between tide gauge and ERS wind driven ocean model (EJSD) simulated sea levels at Jakarta, Jepara, Surabaya and Singapore. The CC and RMSE indicate the correlation coefficient and root mean square error, respectively.

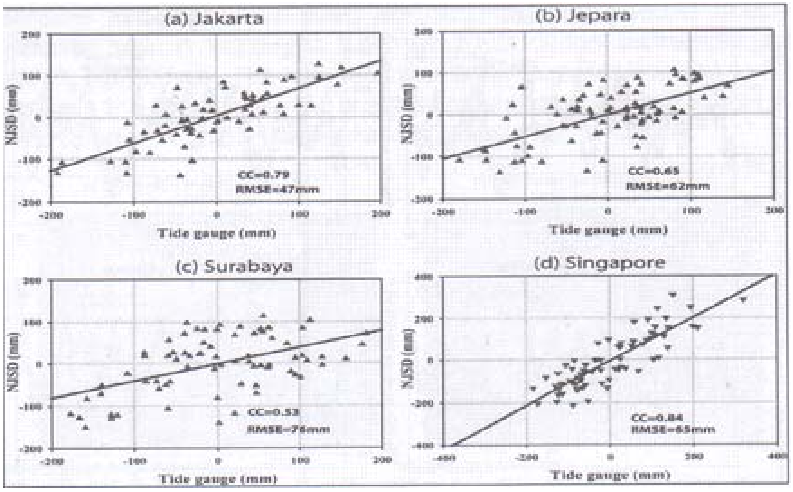

Figure 5: The scatter plot of the comparison between tide gauge and NCEP wind driven ocean model (NJSD) simulated sea levels at Jakarta, Jepara, Surabaya and Singapore. The CC and RMSE indicate the correlation coefficient and root mean square error, respectively.

(a) ERS mean wind field

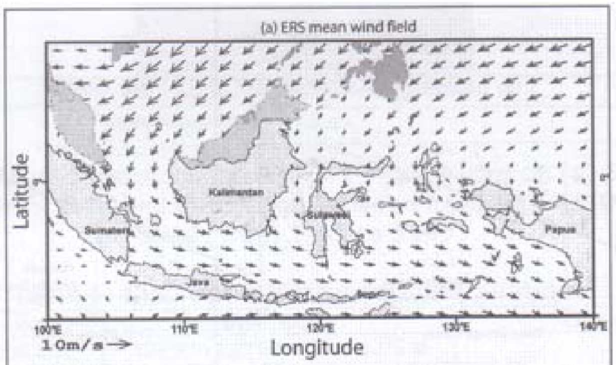

(b) NCEP mean wind field

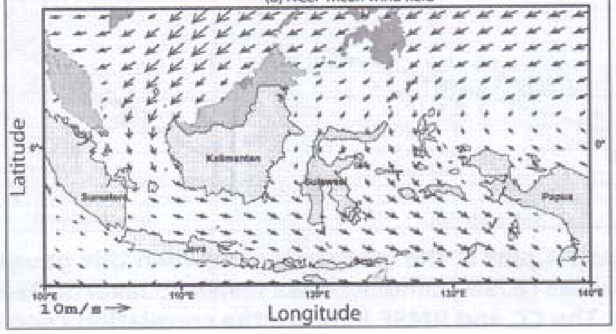

Figure 6. Mean wind vector patterns within the Indonesian Seas during January from 1993 to 1999. The wind vectors are based on (a) ERS and (b) NCEP monthly mean wind fields.

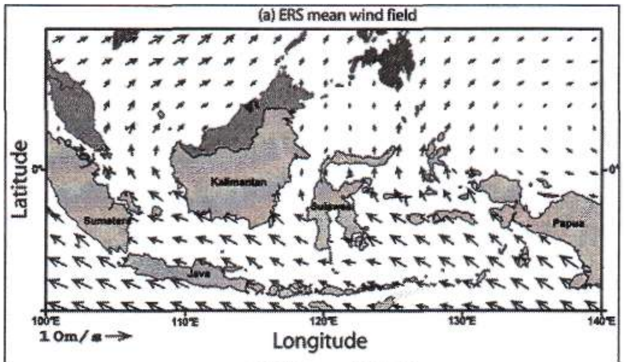
(a) ERS mean wind field

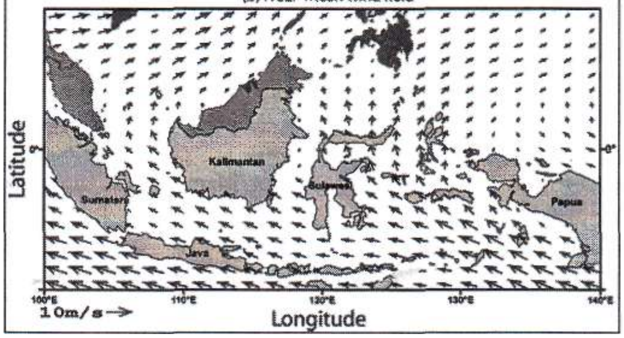
(b) NCEP mean wind field

Figure 7: Mean wind vector patterns within the Indonesian Seas during August from 1993 to 1999. The wind vectors are based on (a) ERS and (b) NCEP monthly mean wind fields.

Model Validation

Figures 2 (a) and (b) show the EJSD and NJSD model-simulated mean sea levels for 7 years from 1993 to 1999. Figure 2 (c) shows the difference between the EJSD and NJSD model-simulated mean sea levels. The EJSD and NJSD model-simulated mean sea levels show similar patterns within the Indonesian Sea. The mean sea level is high at the South China Sea and the Karimata Strait and low at the Java Sea and southern Makassar Strait. The lowest sea level is occurred at south off Java and Sumatera Islands as shown in Figures 2 (a) and (b). The Figure 2 (c) shows the EJSD model-simulated sea level is about 7 cm lower than the one simulated by NJSD model in the Java Sea, and reaches to 7 cm lower at the southern Makassar Strait. Moreover, the EJSD-simulated mean sea level is 5 cm lower than NJSD-simulated sea level in the Sulawesi Sea. On the other hand, the EJSD-model-simulated sea level is 5 cm to 10 cm higher than the one simulated by NJSD model in the South China Sea and Karimata Strait.

These HYCOM-estimated sea levels are validated using tide gauge sea levels. The in-situ sea level data (1993-1999) recorded at Jakarta, Jepara (near Semarang) and Surabaya have been obtained from the National Coordinating Agency for Surveys and Mapping of Indonesia (Bakosurtanal). In addition the tide gauge at Singapore that derived from University of Hawaii Sea Level Center (UHSLC) is also used to validate the simulated mean sea levels at the Karimata Strait. Figures 3, 4 and 5 show the validation results of simulated monthly mean sea levels. The tide gauge and HYCOM show that sea levels are low during the El Nino periods (Figure 3). The results of validation for the BSD model show that correlation coefficients (CC) are ranging from 0.72 to 0.89 and the root mean square errors (RMSE) are varying from 40 mm to 61 mm (Figure 4). On the other hand, the NJSD model-simulated mean sea level has the CC from 0.53 to 0.85 and RMSE from 47 mm to 76 mm (Figure 5). These results indicate that the accuracy of the FJSD model is higher than NJSD model. However, only at Jakarta, the EJSD model-simulated mean sea level has a lower CC and a higher RMSE than NJSD modelled mean sea level. This is probably caused by the lower ERS wind speed and stress than NCEP wind speed and stress at the northern Jakarta (refer to Figures 6 and 7).

On the other hand, according to Sofian et al. [11], the absolute dynamic topography (ADT) derived from various altimeters [12] shows the RMSE from 40 mm to 60 mm against the tide gauge mean sea level. This fact indicates that the accuracies of the two models are comparable with the one derived from ADT.

The signal of ENSO can be seen in both of the model and the tide gauge data at the Java Sea. The tide gauge and simulated sea levels abruptly increase during the transition period from strong El Nino (1997/1998) to strong La Nina (1998/1999), though the simulated sea levels at Jepara and Surabaya tend to be lower than tide gauge sea levels during this period as shown in Figure 3. On the other hand, the signal of ENSO is not clearly seen in both of the model and tide gauge at Singapore. Eventually, the EJSD model shows a better agreement with observation than the NJSD model, in terms of higher CC and smaller RMSE. The summary of validation results between the simulated and tide gauge mean sea levels is depicted in Table 2.

Table 2. Results of validation between the simulated and tide gauge mean sea levels.

Model	Correlation coefficients (CC)				Root mean square error (RMSE)			
	Jakarta	**Jepara**	**Sura baya**	**Singapore**	**Jakarta**	**Jepara**	**Sura baya**	**Singapore**
ERS wind-driven model (EJSD)	0.72	0.85	**0.71**	0.89	**56 mm**	**40 mm**	**61**	**55 mm**
NCEP wind-driven model (NJSD)	0.79	0.65	0.53	0.84	**47 mm**	**62 mm**	**76**	**65 mm**
Altimeter-derived ADT (Sofian et al. [11])	0.75	0.87	0.83	**-**	**60 mm**	**40 mm**	**52**	**-**

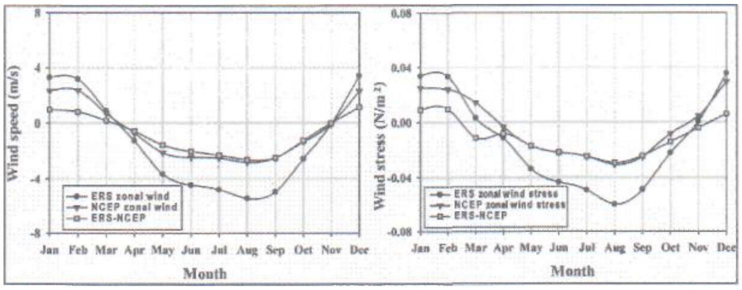

Figure 8: Annual cycles of ERS and NCEP-derived Java Sea zonal wind speed and stress based on 7 years (1993 to 1999) zonal wind data. The positive and negative wind speeds and stresses indicate the westerly and easterly winds, respectively.

Wind Climatology

In this section, wind vector patterns in the Indonesian Sea are compared between ERS and NCEP wind fields. The climate of the Indonesian Sea is characterized by monsoonal winds and high rainfall. Figures 6 and 7 shows the wind vector patterns within ne Indonesian Seas during January and August from 1993 to 1999. The mean wind vector patterns are calculated based on monthly mean ERS and NCEP wind fields. Winds blow *rom the south, curving across the equator with a westward component in the south, and an eastward component in the north, from May to September, the wind direction is nearly opposite during November to March [13]. During the southeast monsoon from May to September, the easterly and southerly winds blow in the Java Sea and the Makassar Strait, respectively. On the other hand, during the northwest monsoon from November to March, wind direction over the Java Sea and Makassar Strait change to westerly and northerly, respectively. In other words, the Java Sea is dominated by the zonal wind throughout the year.

Figures 8 show the ERS and NCEP-derived Java Sea zonal winds (JZW) and wind stresses (JZS). Assuming that the entire JZW and JZS are homogeneous, the JZW and JZS are defined as the average zonal wind and wind stress from 105°E to 115°E and from 7.5°S to 2.5°S. The 7 years means of ERS and NCEP-derived JZW are -1.5 m/s and -0.6 s, respectively. Moreover, the 7 years means of ERS and NCEP-derived JZS are -0.015 N/m^2 and -0.003 N/m^2, respectively. These indicate the JZS tends to be easterly.

The JZW and JZS follow the monsoon seasons. The strongest westerly JZW westerly JZS) and easterly JZW (easterly JZS) occur during January and August, respectively. The westerly ERS JZW is 1.0 m/s higher than the NCEP JZW in December to January. On the other hand, the easterly ERS JZW is 2.5 m/s higher than the NCEP JZW, n August. Similarly, the westerly and easterly ERS JZS are 0.01 N/m^2 and 0.03 N/m^2 higher than NCEP JZS, in December to January and August, respectively. These differences n wind speed and stress can lead to the different surface currents in the Java Sea and the Makassar Strait, which will be discussed in the following sections.

Wind and Surface Current

Figures 9 and 10 show the surface currents based on the EJSD and NJSD models in January (northwest monsoon) and August (southeast monsoon). Generally, the EJSD model-simulated surface current speeds at the Java Sea are 5 cm/s to 10 cm/s faster than NJSD model-simulated one both in January and August. During the northwest monsoon, as the northwesterly wind blows, the monsoonal wind expels the Java Sea water to eastward and the Karimata Strait water to the south. The Sunda Strait surface current is eastward and enters from the Indian Ocean to the Java Sea during this period. Conversely, the wind direction is changed to southeasterly during the southeast monsoon. The wind-driven westward current drives the Java Sea and the Karimata Strait surface waters westward and northward, respectively. The Sunda Strait surface water exits from the Java Sea to the Indian Ocean during the southeast monsoon.

The Makassar Strait current does not follow the monsoonal wind direction. The Makassar Strait surface currents tend to flow southward throughout the year. The southward Makassar Strait surface current speed is low during the northwest monsoon period, though the northerly wind is intensive. The low southward Makassar Strait surface current speed seems to be inhibited by the strong Java Sea eastward current. On the other hand, the southward Makassar Strait surface current speed is getting faster during the southeast monsoon. It is known that, the strong southward Makassar Strait surface current pushes the surface water with low salinity and low temperature back to the Java Sea [5].

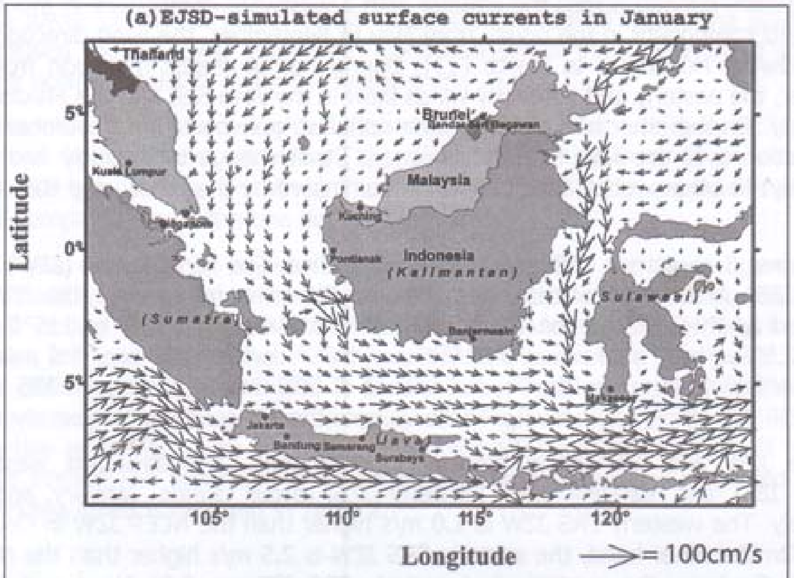
(a) EJSD-simulated surface currents in January

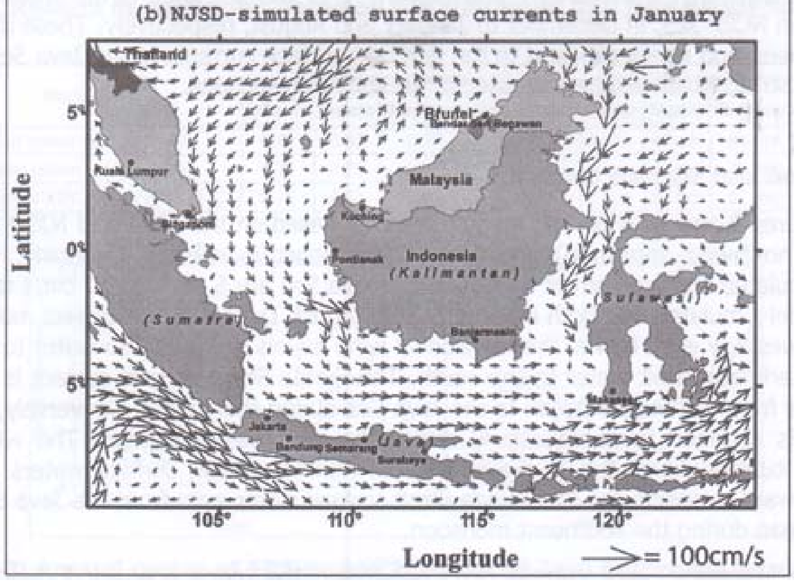
(b) NJSD-simulated surface currents in January

Figure 9: Modelled surface current distributions based on (a) EJSD and (b) NJSD during January from 1993 to 1999.

(a) EJSD-simulated and surface currents in August

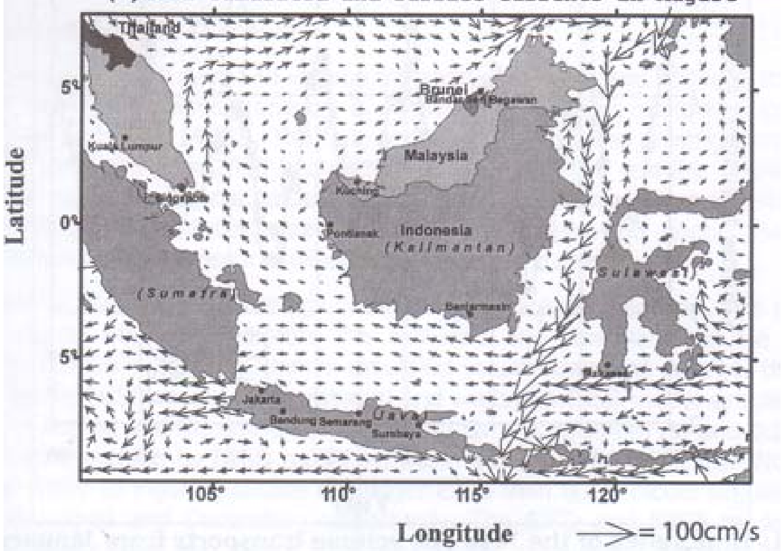

(b) NJSD-simulated surface currents in August

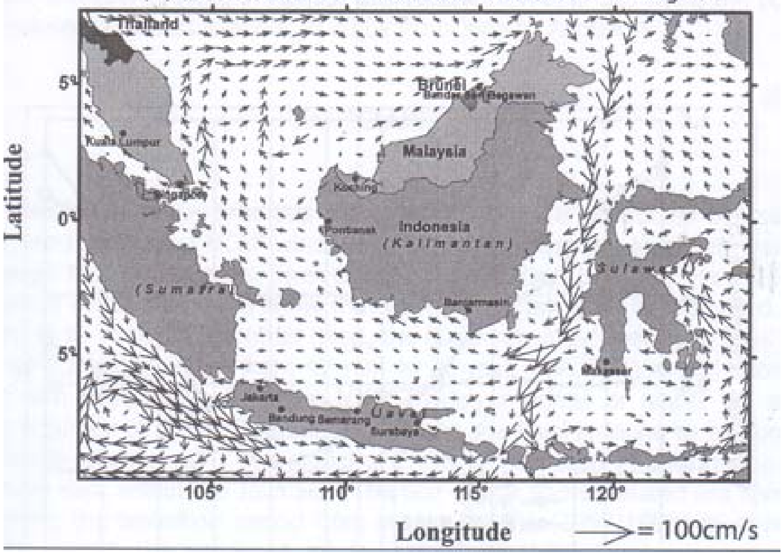

Figure 10: Modelled surface current distributions based on (a) EJSD and (b) NJSD during August from 1993 to 1999.

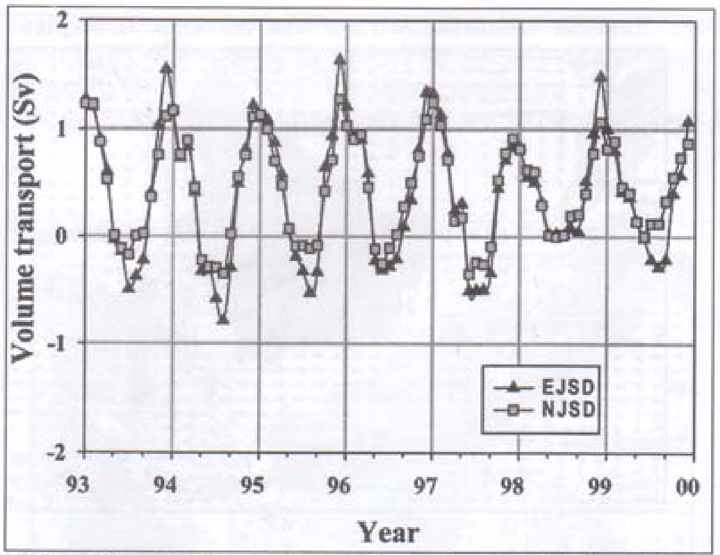

Figure 11: Time series of the Java Sea volume transports from January 1993 to December 1999. The positive volume transport indicates the eastward volume transport. (1 Sv = 1 million m^3/s).

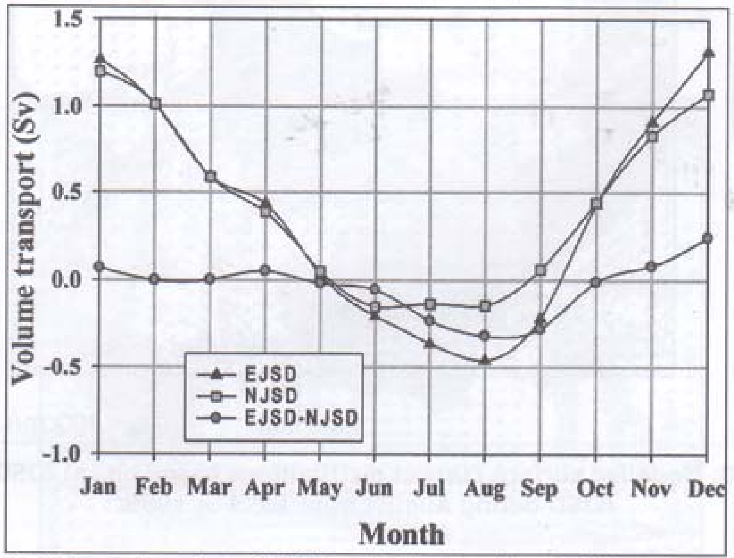

Figure 12: Annual cycles of EJSD and NJSD-estimated Java Sea volume transport based on 7 years (1993 to 1999) volume transport data. The positive and negative volume transports indicate the eastward and westward volume transports, respectively.

Java Sea Volume Transport

In this section, the Java Sea volume transports are compared between the EJSD and NJSD. The Java Sea volume transport is determined from the meridional cross section from 7.0°S to 3.5°S at 114.0°E. The time series of the Java Sea volume transports from January 1993 to December 1999 is depicted in Figure 11. The positive volume transport indicates the eastward volume transport. In general, the Java Sea transport is directed eastward during the northwest monsoon, and to the westward during the southeast monsoon, following the monsoonal wind-induced surface current.

Figure 12 shows the climatology of the Java Sea volume transport. The positive and negative volume transport indicates the eastward and westward volume transports, respectively. Generally, the EJSD model-simulated volume transport is larger than the one simulated by the NJSD model. The eastward and westward EJSD model-simulated volume transports in August and December are 0.30 Sv (1 Sv = 1 million m^3/s) and 0.23 Sv larger than the ones simulated by NJSD model, respectively. The larger ERS than NCEP-derived wind stress (refer to Figures) causes the larger EJSD than NJSD model-simulated volume transport in August and December, respectively. The EJSD and NJSD model-simulated volume transports have two peaks. The peak of the eastward EJSD and NJSD model-simulated volume transports occur in December and January. The peak of the westward EJSD volume transport occurs in August and reaches to -0.48 Sv, while the NJSD model-simulated volume transport is about -0.20 Sv from June to August.

CONCLUSIONS

The simulation of the Java Sea and Makassar Strait is conducted by using HYCOM, which is driven by ERS and NCEP winds. The modelled mean sea levels are validated with the tide gauge mean sea levels. The results of comparison between the EJSD-simulated and tide gauge mean sea levels show that CC ranges from 0.72 to 0.89, and RMSEs are from 40 mm to 61 mm. On the other hand, the NJSD-simulated mean sea level has the CC from 0.53 to 0.84, and RMSE from 47 mm to 76 mm. The EJSD model shows a better agreement with observation than the NJSD model, in terms of higher CC and smaller RMSE. The accuracy of the HYCOM modelled mean sea level is found to be comparable to that of altimeter-derived ADT. The signal of ENSO can be seen in both of the model and the tide gauge data within the Java Sea. The tide gauge and simulated sea levels abruptly increase during the transition period from strong El Nino (1997/1998) to strong La Nina 1998/1999), though the simulated sea levels at Jepara and Surabaya tend to be lower than tide gauge sea levels during this period.

Due to the shallowness of the Java Sea, the volume transport is dominated by the wind. The westerly and easterly ERS wind stresses are 0.01 N/m^2 and 0.03 N/m^2 higher than NCEP wind stresses, in December and August, respectively. Moreover, the ERS mean wind speed is 1.0 m/s and 2.5 m/s higher than NCEP mean wind speed, during the northwest and southeast monsoons, respectively. The model results indicate that the Java Sea eastward volume transport simulated by the EJSD model is larger than the one simulated by the NJSD model. The EJSD model-simulated Java Sea eastward and westward volume transports are 0.23 Sv and 0.30 Sv larger than the ones simulated by the NJDS in December and August, respectively.

Acknowledgement

We thank HYCOM consortium to provide the HYCOM code. The ERS wind data are provided by IFREMER. NCEP wind data are provided by NOAA CDC.

REFERENCES

[I] Gordon, A. L, Susanto, R. D., and Ffield, A., 1999, "Throughflow within Makassar Strait" Geophysical Research Letter, 26, pp. 3325-3328.

[2] Gordon, A. L, and Susanto, R. D., 1999, "Makassar Strait Transport: Initial estimate based on Arlindo Results", J. Marine Technology Society, 32, pp. 34-45.

[3] Ffield, A., Vranes, K., Gordon, A. L, Susanto, R. D., and S. L Garzoli , 2000, "Temperature Variability within Makassar Strait", Geophysical Research Letter, 27, 237-240.

[4] Waworuntu, J., Fine,R., Olson, D., and A. L. Gordon, 2000, "Recipe for Banda Sea water", J. Marine Research, 58, pp. 540-570.

[5] Gordon, A. L., Susanto, R. D., and Vranes, K., 2003, "Cool Indonesian throughflov. as a consequence of restricted surface layer flow", Nature, 425, pp. 824-828.

[6] Sofian, I., Kozai, K., and Ohsawa, T, 2006, "Investigation on the interoceanic connection between the Makassar Strait and the Java Sea", Proceedings of Techno-Ocean 2006/19* JASNAOE Ocean Engineering Symposium, Paper No. 90.

[7] Sofian, I., Kozai, K., and Ohsawa, T., 2007, "Investigation on the relationship between wind-induced transport and mean sea level in the Java Sea using an oceanic general circulation model", UMITOSORA, in press.

[8] Bleck, R., 2002, "An oceanic general circulation model framed in hybrid isopycnic-cartesian coordinates", Ocean Modeling, 58, pp. 547-569.

[9] Large, W. G., McWilliams, J. C, and Doney, S. C, 1994, "Oceanic vertical mixing: a review and a model with nonlocal boundary layer parameterization", J. Rev. Geophys, 32, pp. 363-403.

[10] CERSAT-IFREMER, 2002, "Mean Wind Field (MWF Products) Volume 1, ERS-1, ERS2 and NSCAT user manual", version 1.0, C2-MUT-W-05-IF

[II] Sofian, I., Kozai, K., and Ohsawa, T., 2006, "Estimation of the sea level variations of the Java Sea using the HYCOM", the International Pan Ocean Remote Sensing Conference, Busan, Korea.

[12] AVISO, 2004, "(M)SLA and (M)ADT Near-Real Time and Delayed Time Products Handbook", edition 1.2.

[13] Tomczak, M. and Godfrey, J. S., 2001, "Regional Oceanography: an introduction", online edition, PDF version 1.0, pp. 220-228.